Structural dynamics and oligomeric interactions of Na^+,K^+-ATPase as monitored using fluorescence energy transfer

Evzen Amler, Alan Abbott, and William James Ball, Jr.
Department of Pharmacology and Cell Biophysics, University of Cincinnati College of Medicine, Cincinnati, Ohio 45267-0575 USA

ABSTRACT The oligomeric nature of the purified lamb kidney Na^+,K^+-ATPase was investigated by measuring the fluorescence energy transfer between catalytic (α) subunits following sequential labeling with fluorescein 5'-isothiocyanate (FITC) and erythrosin 5'-isothiocyanate (ErITC). Although these two probes had different spectral responses upon reaction with the enzyme, our studies suggest that a sizeable proportion of their binding occurs at the same ATP protectable, active site domain of α. Fluorescence energy transfer (FET) from donor (FITC) to acceptor (ErITC) revealed an apparent 56 Å distance between the putative ATP binding sites of α subunits, which is consistent with $(\alpha\beta)_2$ dimers rather than randomly spaced $\alpha\beta$ heteromonomers. In this work, methods were introduced to eliminate the contribution of nonspecific probe labeling to FET values and to determine the most probable orientation factor (K^2) for these rigidly bound fluorophores. FET measurements between anthroylouabain/ErITC, 5'-iodoacetamide fluorescein (5'IAF)/ErITC, and TNP-ATP/FITC, donor/acceptor pairs were also made. Interestingly, none of these distances were affected by ligand-dependent changes in enzyme conformation. These results and those from electron microscopy imaging (Ting-Beall et al. 1990. *FEBS Lett.* 265:121) suggest a model in which ATP binding sites of $(\alpha\beta)_2$ dimers are 56 Å apart, and reside 30 Å from the intracellular surface of the membrane contiguous with the phosphorylation domain.

INTRODUCTION

The Na^+,K^+-ATPase (EC 3.6.1.3) is a plasma membrane-bound enzyme that actively maintains the cellular transmembrane electrochemical gradients of Na^+ and K^+. The enzyme consists of at least two major subunits: the catalytic α subunit (MW $\cong$ 112,000) and the associated glycoprotein β subunit (MW $\cong$ 35,000, excluding oligosaccharides). There may also be a low molecular weight polypeptide or proteolipid component, γ ($M_r \cong$ 6700), associated with the enzyme. While no actual catalytic function for β has been demonstrated and the presence and role for γ is even less certain, there is general agreement that the two major subunits are associated at a 1:1 ratio and that both are required for function (see reviews by Pedemonte and Kaplan, 1990; Jørgensen, 1982; McDonough et al., 1990).

The ATP-driven Na^+ and K^+ translocation processes have been examined extensively yet the details of how ATP hydrolysis is physically coupled with the structural changes in the enzyme that must occur in order to regulate the cation flux is not understood. The enzyme undergoes a sequence of conformational changes that alters the spatial relationships between the cation and ATP binding sites and the phosphorylation site. However, estimates of these distances and how they change are at best tentative. In addition, there is no clear understanding of the minimal functional unit associated with ATP hydrolytic activity, ion transport, and regulation (Jørgensen and Anderson, 1988).

A variety of biophysical approaches have been used to investigate the functional assembly of the enzyme. Radiation inactivation studies have in general reported a target size for the Na^+,K^+-ATPase activity that is greater than the sum of an α and β subunit pair (Ottolenghi and Ellory, 1983; Cavieres, 1988). For example, recent studies of Nørby and Jensen (Nørby and Jensen, 1989; Jensen and Nørby, 1989) using frozen enzyme have suggested that the inactivation size of the enzyme for nucleotide, vanadate, and ouabain binding and K^+-pNPPase activity is close to the mass of only 112 kD, while the Na^+,K^+-ATPase activity and Tl^+ occlusion have apparent molecular weights of ~195 kD, thus suggesting that an α_2 dimer (195 kD) serves as the functional unit with β playing no role in catalysis. Low-angle neutron scattering analysis of the kidney enzyme dissolved in the detergent Brij (Pachence, et al., 1987) has suggested that an $\alpha_2\beta_2$ heterodimer is the functional unit.

Other laboratories have, though, demonstrated in the

Address correspondence to Dr. Ball.
Dr. Amler is on leave from the Institute of Physiology, Czechoslovak Academy of Sciences, Prague, Czechoslovakia.

Abbreviations: AO, 9-anthroylouabain; ErITC, erythrosin-5'-isothiocyanate; 5'-IAF, 5'-iodoacetamidofluorescein; KLH, keyhole limpet haemocyanin; MOPS, 3-[*N*-morpholino] propanesulfonic acid; Pipes, piperazine-*N*,*N*'-*bis* [2-ethenesulfonic acid]; TNP-ATP, 2',3'-0-(1,4,6-trinitrocyclohexadienylidine) adenosine-5'-triphosphate; FET, fluorescence energy transfer.

0006-3495/92/02/553/16 $2.00

non-ionic detergent dodecyl octaethylene monoether ($C_{12}E_8$) the presence of active αβ protomers as well as $(\alpha\beta)_2$ diprotomers (Brotherus et al., 1983; Hayashi et al., 1989). While negative staining and computer enhanced electron microscopy imaging of two dimensional crystalline arrays of the membrane embedded enzyme show that there are both αβ and associated $(\alpha\beta)_2$ dimeric arrays depending upon the exact crystallization conditions (Skriver et al., 1981; Zampighi et al., 1984; Beall et al., 1989).

The use of Forster energy transfer measurements between donor and acceptor fluorophores labeling the ATPase provides an additional means of investigating both conformational changes in the enzyme and its quaternary structure. While efforts with the Na^+,K^+-ATPase have largely focused upon measurements of distances between fluorophores labeling different sites on α or between α and β (Jesaitis and Fortes, 1980; Lee and Fortes, 1986; Fortes and Aquilar, 1988), efficient energy transfer between sarcoplasmic reticulum Ca^{2+}-ATPase monomers has been reported which suggests substantial oligomeric interactions (Gingold et al., 1981; Watanabe and Inesi, 1982; Papp et al., 1987).

In these studies we have made extensive use of fluorescein-5′-isothiocyanate (FITC) and the tetraiodinated fluorescein derivative erythrosin-5′-isothiocyanate (ErITC) as the donor and acceptor pair to make structural and dynamic measurements of α–α interactions. These fluorophores were chosen because they have a significant spectral overlap giving an efficient energy transfer suitable for long range interactions and similar structures which suggested that they should be directed to the same reactive groups on Na^+,K^+-ATPase. FITC has been used extensively and shown to largely covalently label α at a site (Lys-501), which places the probe in the vicinity of the ATP binding domain and makes its fluorescence intensity sensitive to conformational changes in the enzyme (Farley et al., 1984; Xu, 1989; Karlish, 1980; Friedman and Ball, 1989; Taniguchi et al., 1988). We have found that ErITC, like FITC, reacts with and inhibits the Na^+,K^+-ATPase activity with ATP protecting against this inactivation, but unlike FITC it does not show conformation-dependent changes in its fluorescence intensity. Using Forster energy transfer determinations we have measured the intra-α distances between anthroylouabain and ErITC, between 5′-IAF and ErITC, and between 5′-IAF and TNP-ATP binding or labeling sites. We have also measured the energy transfer distance between α subunits using ErITC- and FITC-labeled enzyme. The latter work required consideration of both specific and nonspecific components of the probes' labeling stoichiometries (Abbott et al., 1991) and the highly restricted rotational motion of FITC and ErITC, which effects the value of the orientation factor (K^2) used in the distance calculations.

MATERIALS AND METHODS

Na^+,K^+-ATPase isolation and characterization. The Na^+,K^+-ATPase was purified from the outer medulla of frozen lamb kidney by the method of Lane et al. (1979). The initial activity of the enzyme after purification varied from 800–1,100 μmol ATP hydrolyzed/mg protein/h as assayed spectrophotometrically according to Schwartz et al. (1969). The protein concentration was determined by the Lowry procedure (Lowry et al., 1951) and then reduced by a 1.4 factor in order to correct for the Lowry's protein overestimate (Moczydlowski and Fortes, 1981). The protein purity was confirmed by PAGE (Laemli, 1970), and the FITC labeling of α was visualized in the gels using a Spectroline model TL-33 UV transilluminator (UVP Inc., San Gabriel, CA). The proteins were visualized in the gel by Coomassie brilliant blue staining.

Fluorescent probe labeling of enzyme. FITC and ErITC labeling of the enzyme was accomplished by adding the probe, freshly dissolved in DMSO, to the enzyme (1 mg/ml, in 50 mM Tris/HCl, pH 9) at room temperature, in the dark for 30 min. The DMSO concentration with the enzyme was kept below 0.5%. The reactivity of unbound fluorophore was quenched by the addition of 40 μM mercaptoethanol and dilution of the reaction solution. The labeled sample was then gel filtered through a 10-fold volume excess of Sephadex G-50 using a desk top centrifuge unless otherwise stated. The 5′-IAF labeling was done according to the procedures of Tyson et al. (1989). The enzyme (1.5 mg/ml) pretreated with 25 mM iodoacetate at 37°C for 30 min, in 50 mM imidazole-HCl, 20 mM KCl, pH 7.5 was then incubated in the dark for 24 h with 200 μM 5′-IAF. The iodoacetate and 5′-IAF were removed by Sephadex G-50 gel filtration.

Steady-state fluorescence measurements. All steady-state fluorescence intensity measurements were performed on an SLM/Aminco SPF-500C spectrofluorometer. The excitation light was vertically polarized and the emission was observed either under magic angle conditions or through a polarizer oriented vertically (I_v) and then horizontally (I_h) relative to the excitation light. In the later case, fluorescence intensity was calculated as $I = I_v + 2I_h$. The steady-state anisotropy values r were calculated according to the equation:

$$r = [(I_v/I_h)G - 1]/[(I_v/I_h)G + 2], \quad (1)$$

where the instrument factor, G, equals I_h/I_v when the excitation light is oriented horizontally and effectively corrects r for unequal detection of vertically and horizontally polarized light.

Anthroylouabain (AO) binding and quantitation. The enzyme (both unlabeled and labeled with ErITC) was incubated with AO for 20 min in 50 mM Tris, 5 mM $MgCl_2$, and 5 mM P_i, at 37°C. The AO binding and quantitation of total number of enzyme binding sites was determined according to Fortes (1986).

Iodide quenching analysis. Iodide ions were used for collisional quenching of FITC and ErITC covalently linked to Na^+,K^+-ATPase. All titrations were performed in triplicate and the quenching constants K_q were derived from the slope of the line with the data plotted using the Stern-Volmer equation:

$$F_0/F = 1 + K_q[Q], \quad (2)$$

where F_0 and F are the fluorescence intensities of the fluorophore in the presence and absence of quencher and $[Q]$ is the molar concentration of quencher.

Dynamic measurements of fluorescence lifetimes. Fluorescence decay lifetimes of the excited state of FITC were measured using the phase

and modulation technique (Spencer and Weber, 1969). Measurements over the modulation frequency range of 10–200 MHz were made using an SLM 4800 fluorometer modified with a Pockel cell modulator (I.S.S. Inc., IL) as described previously by Mclean et al. (1989). The exciting light λ = 485 nm was achieved with the monochromator and the emission was observed through a bandpass interference filter (center, 520 nm; bandwidth, 7 nm). Measuring the lifetime of ErITC with its short lifetime required the use of a newly designed system that allows the generation of modulation frequencies up to 10 GHz (Laczko et al., 1990). The excitation wavelength of 514 nm was generated by an Argon Ion (Inova 15; Coherent, CA) mode locked laser. The detector was a Hamamatsu R2566, 6μ photomultiplier. An aqueous suspension of LUDOX in water was used as a reference sample. The data were collected using a DEC PDP 11/23 computer and then transferred to a DEC PDP 11/73 (Digital Equipment Corp.) for analysis in terms of the sum of exponentials of fluorescence decay as described previously (Lakowicz et al., 1984) using a nonlinear least-squares method for multiexponential fitting. The reduced χ^2 parameter was used to judge the quality of the fit:

$$\chi_R^2 = \frac{1}{\gamma}\sum_{\omega}\left(\frac{\phi_\omega - \phi_{c\omega}}{\delta\phi}\right)^2 + \frac{1}{\gamma}\sum_{\omega}\left(\frac{m_\omega - m_{c\omega}}{\delta m}\right)^2, \quad (3)$$

where γ is the number of degrees of freedom and δ_ϕ and δ_m are the experimental uncertainties in the measured phase (ϕ) and modulation (m) values. For all analyses, the uncertainties in the phase and modulation measurements were taken as 0.2 and 0.005, respectively. This latter work was done under the direct supervision of Drs. J. Lakowicz and H. Malak and used the software available at the center for Fluorescence Spectroscopy, University of Maryland School of Medicine, Baltimore.

Forster energy transfer (FET) measurements. Calculated distances (R) between donor and acceptor pairs were derived from the Forster energy transfer measurements. The apparent efficiency of transfer E, was calculated by determining either the extent of quenching of the donor's fluorescence intensity or the decrease in donor decay lifetime as shown in Eq. 4:

$$E = 1 - F/F_0 = 1 - \tau/\tau_0, \quad (4)$$

where F and F_0 are fluorescence intensities, and τ and τ_0 are the lifetimes of donor in the presence and absence of acceptor, respectively (Lakowicz, 1983). The apparent efficiency, E, of the energy transfer is related to the absolute rate of energy transfer k_t as given below:

$$E = (k_t\tau_0)/(1 + k_t\tau_0) \quad (5)$$

and this rate has been defined by Forster (1951):

$$k_t = (\Phi J K^2/\tau_d n^4 R^6) \times 8.7 \times 10^{23} S^{-1}, \quad (6)$$

where Φ and τ_d are the quantum yield and lifetime, respectively, of the donor in the absence of acceptor, n is the refractive index of the solution, R is the distance between donor and acceptor (in centimeters), J is the spectral overlap integral (cm^3/M) defined as:

$$J = \frac{\int F_d(\lambda_{ex}, \lambda)\epsilon_A(\lambda)\lambda^4\, d\lambda}{\int F_d(\lambda_{ex}, \lambda)\, d\lambda}, \quad (7)$$

where $\epsilon_A(\lambda)$ is the extinction coefficient of the acceptor and $F_d(\lambda_{ex}, \lambda)$ is the fluorescence of the donor (excited at λ_{ex}) that is emitted at wavelength λ. Finally, K^2 is the orientation factor of the donor which is defined as:

$$K^2 = (\sin\alpha \sin\beta \cos P - 2\cos\alpha\cos\beta)^2, \quad (8)$$

and α and β are, respectively, the angles that the donor's emission dipole and the acceptor's absorption dipole, form with vector **R**. Vector **R** connects these two dipoles. P then is the angle between the planes which contain α and β. By substituting Eq. 6 into Eq. 5, and setting energy transfer efficiency (E) to 0.5, the resulting "Forster distance" is $R_0^6 = 8.7 \times 10^{23}\, \Phi J K^2/n^4$. Furthermore, since the orientation factor K^2 was not constant (or 2/3) for all measurements, R_0 was defined in terms of the "critical distance," R_c, and the orientation factor K^2 ($R_0^6 = R_c^6 K^2$). Then from Eqs. 5 and 6 we can obtain the following:

$$1 - E = 1/(1 + K^2 R_c^6/R^6). \quad (9)$$

Substituting Eq. 9 into Eq. 4 the distance between the donor and acceptor pairs was calculated upon determination of the R_c values, the efficiency of the energy transfer and assuming a value for K^2:

$$R = R_c[FK^2/(F_0 - F)]^{1/6} = R_c(1/E - 1)^{1/6} K^{2/6}. \quad (10)$$

For several of the fluorophores used (5′-IAF, AO, and TNP-ATP), we assumed there was random orientation of the probe during its lifetime and we took K^2 = 2/3 (Dale and Eisinger, 1976). In the case of FITC and ErITC, which both have a high level of restriction ($r > 0.30$), the K^2 value was corrected using a modification of the analysis of Dale and Eisinger (1974) and Haas et al. (1978) as presented in Results.

For determination of the overlap integrals (J), the following values of extinction coefficients (ϵ) and quantum yields (Φ) were used: FITC and 5′IAF, $\epsilon = 7.2 \times 10^4\, M^{-1}\, cm^{-1}$, ϕ = 0.4; ErITC, $\epsilon = 8.8 \times 10^4\, M^{-1}\, cm^{-1}$; AO, ϕ = 0.2; LY, $\epsilon = 1.2 \times 10^4\, m^{-1}\, cm^{-1}$, ϕ = 0.18. The J value determined for FITC/ErITC and 5′-IAF/ErITC was the same, $4.6 \times 10^{-13}\, cm^3/M$; for AO/ErITC, $1.94 \times 10^{-13}\, cm^3/M$; while that for 5′-IAF/TNP-ATP, $1.2 \times 10^{-14}\, cm^3/M$ was obtained from Fortes and Aquilar (1988).

MATERIALS

The fluorescent probes, FITC, AO, TNP-ATP, and 5′-IAF were purchased from Molecular Probes (Eugene, OR), and ErITC was purchased from Sigma Chemical Co. (St. Louis, MO). The anti-FITC antibodies were affinity purified, rabbit polyclonal IgG kindly supplied by Dr. E. W. Voss, Jr. (University of IL, Urbana). All other chemicals were of enzyme or analytical grade.

RESULTS

ErITC labeling and inactivation of Na^+,K^+-ATPase. The purified lamb kidney enzyme was labeled with 4–20 μM ErITC for 30 min in the absence and presence of 10 mM ATP. Comparison of the effects of ErITC and FITC on enzyme activity showed ErITC to be the more effective inhibitor and its inactivation somewhat less protected by ATP (Table 1). There does remain some question as to whether ErITC has a higher binding affinity, or if the higher level of inhibition results at least partially from the nonspecific labeling that occurred even in the

TABLE 1 **Determination of the effects of varying FITC and ErITC concentrations on enzyme activity and the protective effects of ATP**

Labeling concentration:	(in μM) 4	6	10	20
Reactant	% Enzyme activity remaining			
FITC (−ATP)	45 ± 9	28 ± 4	13 ± 5	3 ± 1
FITC (+ATP)	80 ± 10	72 ± 16	77 ± 8	60 ± 7
ErITC (−ATP)	26 ± 14	13 ± 9	9 ± 7	8 ± 3
ErITC (+ATP)	74 ± 3	69 ± 9	59 ± 2	39 ± 3

The FITC Na^+,K^+-ATPase (1 mg/ml) was incubated with 4, 6, 10, and 20 μM FITC or ErITC, respectively, without (−ATP) and with (+ATP) 10 m*M* ATP present. The enzyme activity is given as a percentage of the activity remaining compared with that of untreated enzyme. The data result from four independent experiments done in triplicate.

presence of ATP or from ErITC-dependent photooxidation of functionally important −SH or $-NH_2$ groups. We have observed that exposure of ErITC-labeled enzyme to incandescent light for 30 min resulted in a 50% decrease in activity that did not occur with either FITC- or ErITC-labeled samples kept in the dark. This decrease in enzyme activity was observed whether or not ATP was present. In terms of its labeling stoichiometry at 8 and 10 μM concentrations, 6.4 and 8 nmol/mg of probe was bound to the enzyme, respectively. This was somewhat higher than that observed for FITC. In order to verify that ErITC and FITC competed for the same binding sites, we then prelabeled the enzyme with FITC (1 μM/μM enzyme) and then labeled with ErITC. Monitoring the fluorescence intensity of the ErITC (Table 2) showed that FITC treatment reduced ErITC labeling by 57%, and that ATP reduced the labeling by 52%. Also, ATP did not cause any additional reduction in ErITC labeling if the enzyme was already exposed to FITC. This suggested that ~60% of the ErITC labeling was at the same site as FITC or ATP, but that there was also substantial labeling at a "nonspecific site" which was not saturated by the pretreatment with FITC. This "nonspecific" labeling component is very likely similar to that observed in our earlier work with FITC (Abbott et al., 1991). In a somewhat analogous manner we could also show that prelabeling of the enzyme with ErITC before addition of FITC substantially reduced the fluorescence of FITC-labeled α (as observed upon SDS-polyacrylamide gel electrophoresis, see Fig. 1, *a* and *b*). Because there was the possibility that the FITC fluorescence was reduced by Forster energy transfer from FITC to ErITC, we also used the Western blotting technique to quantitate enzyme bound FITC. In this experiment, one sample of enzyme was labeled with 8 μM ErITC and then this sample and a control were labeled with 10 μM FITC. After removal of free probe, both samples were subjected to gel electrophoresis, electroblotting onto nitrocellulose, and exposure to anti-FITC antibodies to quantitate the level of bound FITC. Fig. 1 *c* shows that

TABLE 2 **Determination of the protective effect of ATP upon ErITC labeling of native and FITC-labeled enzyme**

ATP concentration	Relative labeling of Na^+,K^+-ATPase by ErITC: Na^+,K^+-ATPase	FITC-Na^+,K^+-ATPase
	(*a.u.*)	(*a.u.*)
0 mM	100 ± 3%	43 ± 4%
3 mM	67 ± 2%	43 ± 5%
10 mM	48 ± 4%	44 ± 3%

The FITC-Na^+,K^+-ATPase (1 mg/ml) was pretreated with 10 nmol FITC/mg and subsequently native and FITC-enzyme was labeled in the absence or in the presence of increasing concentrations of ATP, with 8 nmol ErITC/mg protein (see Methods). After removal of unreacted probe, the fluorescence intensity of ErITC-labeled Na,K-ATPase was measured (λ_{ex} = 535 nm, λ_{em} = 558 nm). The average values given in relative fluorescence units (a.u.) and standard deviations were calculated from three measurements.

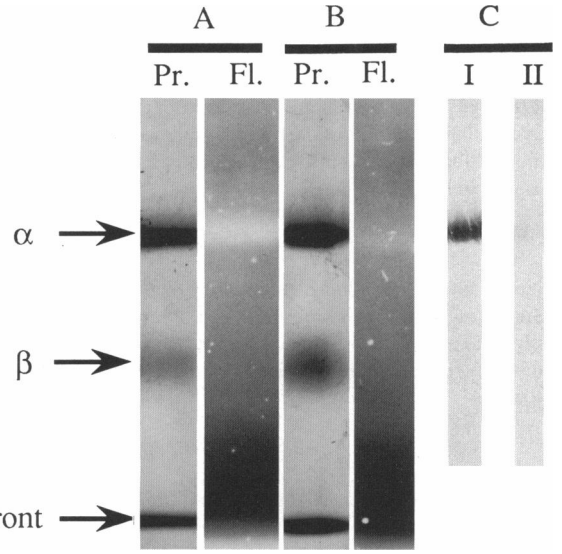

FIGURE 1 SDS gel electrophoresis and Western blot analysis of FITC and ErITC labeling of the α-subunit. (*A* and *B*) The strips show SDS PAGE of FITC-only labeled Na^+,K^+-ATPase (lanes *1*, *2*) and FITC-enzyme prelabeled with 8 μM ErITC (lanes *3*, *4*). The Coomasie Blue-stained proteins are shown in lanes *1*, *3* (Pr.) and the fluorescence emission patterns (Fl.) in lanes *2*, *4*. The same samples were stained after taking the fluorescence emission pictures. (*C*) Western blot analysis of fluorophore labeled enzyme with anti-FITC antibody. Lane *I* shows quantitation of enzyme bound FITC for FITC-Na^+,K^+-ATPase and lane II that for FITC-labeling after prelabeling with 8 μM ErITC.

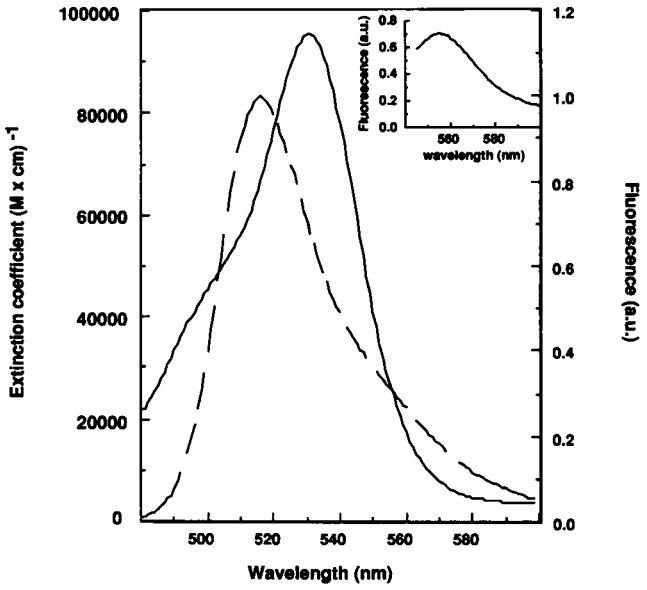

FIGURE 2 Determination of the overlap of the fluorescence emission spectra of FITC-Na^+,K^+-ATPase and the absorption spectra of ErITC-Na^+,K^+-ATPase. The ErITC-Na^+,K^+-ATPase absorption (*solid line*, λ_{max} = 535), FITC-Na^+,K^+-ATPase fluorescence emission (*broken line*, λ_{max} = 520 nm) and ErITC-Na^+,K^+-ATPase fluorescence emission (*inset*, λ_{max} = 555 nm) spectra were obtained in a 10 mM Tris-HCl, 1 mM EGTA, pH 7.4 buffer. The enzyme was labeled as described in the Methods. The reagent concentrations for labeling were 10 μM/mg protein. The final protein concentration for fluorescence records was 10 μg/ml.

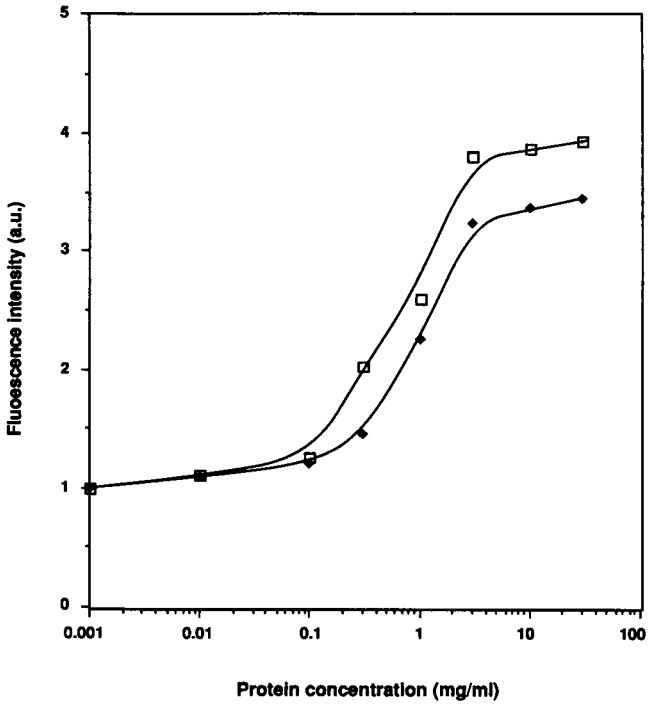

FIGURE 3 Determination of the enhancement in ErITC fluorescence intensity after binding to Na^+,K^+-ATPase. Increasing concentrations of Na^+,K^+-ATPase were incubated with a constant (8 μM) concentration of ErITC in the absence (□) and presence (▲) of 10 mM ATP. Excitation wavelength λ_{ex} = 535 nm, emission wavelength λ_{em} = 558 nm.

ErITC indeed prevented the stable covalent labeling of α by FITC.

Characterization of the fluorescence properties of ErITC. Next we characterized the fluorescence properties of both free and enzyme-bound ErITC in order to better determine the influence of solvent and the protein environment upon the probe and compare these results with those of FITC. As shown in Fig. 2 the absorption spectrum of ErITC-Na^+,K^+-ATPase overlaps substantially with the emission spectrum of FITC-Na^+,K^+-ATPase. This overlap combined with the high quantum yield of FITC and high extinction coefficient of ErITC make the FITC/ErITC pair suitable for FET measurements. These spectra as well as the emission spectrum of ErITC (Fig. 2, *inset*) showed no dramatic wavelength shifts after enzyme labeling. There was however a substantial increase in the relative quantum yield of ErITC. Fig. 3 shows the titration of 8 μM ErITC with increasing concentrations of enzyme. At saturating levels of enzyme the ErITC fluorescence leveled off after a fourfold increase. Because this increase could not be specifically attributed to probe labeling at the ATP protectable site, the same experiment was repeated in the presence of ATP. In this case there was approximately a 3.5-fold increase in fluorescence. Apparently, the difference between specific and nonspecific labeling with respect to the fluorescence increase was small. This result differed from that observed with FITC which showed a site-specific twofold reduction of its fluorescence quantum yield upon labeling the enzyme.

It appears that the increase in the ErITC quantum yield results from some aspect of the probe's interaction with its immediate protein and solvent environment. In going from an aqueous, polar solvent to increasingly nonpolar solvents, we find that the fluorescence intensity of free ErITC (Fig. 4, *inset*) is enhanced and undergoes a red shift in the emission spectrum. This data suggests that the enzyme-linked probe resides in a nonpolar environment that enhances the fluorescence without any significant red shift. It is not quite that simple though, since the spectral properties of this probe are also modified by specific interactions. As shown in Fig. 4, relatively low (5%) concentrations of dimethylformamide added to aqueous buffer (a concentration too low to alter the general properties of the solvent) can

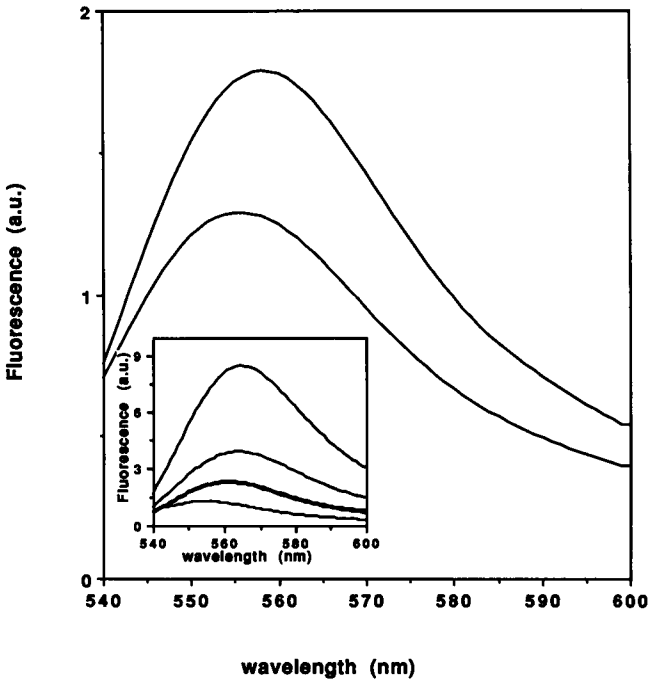

FIGURE 4 The effect of solvent polarity upon the ErITC fluorescence emission spectrum. The ErITC (100 nM) fluorescence emission spectra were taken in 50 mM Tris-HCl, 1 mM EGTA, pH 7.4 before (*lower line*) and after (*upper line*) addition of dimethylformamide (5%). (*Inset*) The ErITC fluorescence emission spectra in (in order from the bottom) TRIS buffer (100 nM ErITC), methanol (50 nM ErITC), ethyleneglycol (50 nM ErITC), propanol (20 nM ErITC), and dimethylformamide (20 nM ErITC), respectively. The excitation wavelength was 535 nm.

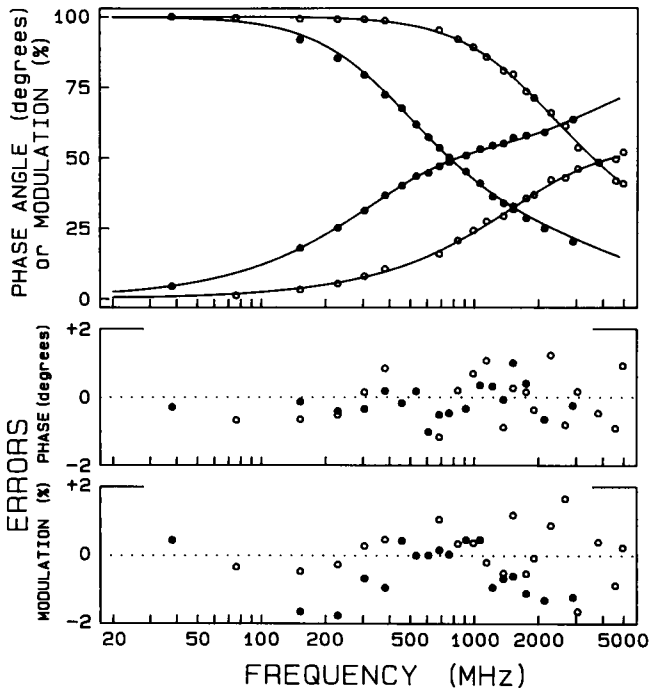

FIGURE 5 The Frequency-domain response of ErITC emission in buffer and after binding to Na^+,K^+-ATPase. Free ErITC (20 μM in 100 mM Tris-HCl, 1 mM EGTA, pH 7.4) (○, *open circle curves*) and bound ErITC-Na^+,K^+-ATPase (1 mg prot/ml) (●, *closed circle curves*) was excited by an Argon Ion mode-locked laser (1 W at 514 nm; Coherent, IL) over a modulated 40 MHz-5 GHz frequency range, and the emitted fluorescence was isolated using a Schott 3-67 filter. The lower two panels show the errors in the collected phase and modulation data, respectively. The ErITC labeling concentration was 8 μM.

enhance the probe's fluorescence and evoke a red shift in the emission spectra.

Since the fourfold fluorescence intensity increase should reflect an increased lifetime (τ) of the probe's excited state, we used a multifrequency phase resolved fluorometer which is capable of generating modulation frequencies up to 10 GHz (Laczko et al., 1990) to determine ErITC's decay lifetime. The phase and modulation responses for both free and enzyme linked probe are shown in Fig. 5 and then analyzed results tabulated in Table 3. The fluorescence emission decay curves were complex and best fit by a double-exponential model for both cases. While the average lifetime for the free probe was very short (τ = 73 ps), it increased 4.8 times to τ = 352 ps upon binding to the enzyme. Interestingly, the fractional contributions of, or distribution of, the decay curve between a shorter and longer lifetime component was essentially unchanged whether the probe was bound or free. In both cases the probes longer lived component contributed more than 80% of the total steady-state intensity. The fact that the increase in the observed lifetime was actually ~20% higher than the enhancement of steady-state fluorescence suggested that there was some static quenching of ErITC upon binding to the enzyme as well as an increased lifetime.

Also, the probe is rotationally quite restricted within the nanosecond and picosecond time scales as evidenced by the fact that the steady-state anisotropy of ErITC was found to be relatively high and the same for both free or bound probe (r = 0.31). In addition, measurements of the time-resolved decay of anisotropy of the bound probe as obtained from frequency-domain measurements showed little shift of the phase angle differences between the parallel and perpendicular components of polarized emission (less than 3 degrees) over a 1 MHz to 5 GHz range.

ErITC sensitivity to conformational changes. Although FITC and ErITC are similar fluorescent molecules with the same chemically reactive group, their fluorescence responses to ligand-induced conformational changes in the enzyme differed. While FITC-labeled Na^+,K^+-ATPase showed an ~24% decrease in fluorescence

TABLE 3 **Lifetime analysis of the excited state of free ErITC and after Na^+,K^+-ATPase bound ErITC**

Number of lifetimes		Analysis parameters				
		τ_i (ns)	α_i	f_i	$\langle\tau\rangle$ (ns)	χ^2
ErITC (in buffer)						
1	τ_1	0.063	1.0	1.0	0.063	158.9
2	τ_1	0.009	0.65	0.17		
	τ_2	0.086	0.35	0.83	0.073	4.1
3	τ_1	0.009	0.65	0.17		
	τ_2	0.085	0.20	0.46		
	τ_3	0.088	0.15	0.37	0.073	4.3
ErITC-Na^+,K^+-ATPase						
1	τ_1	0.261	1.0	1.0	0.261	457.1
2	τ_1	0.059	0.59	0.17		
	τ_2	0.412	0.41	0.83	0.352	2.5
3	τ_1	0.049	0.54	0.14		
	τ_2	0.226	0.17	0.19		
	τ_3	0.461	0.29	0.67	0.359	1.8

Fluorescence lifetimes of the excited state of ErITC (20 μM) in 100 mM Tris-HCl, 1 mmol/l EGTA, pH 7.4 were measured on a 10 GHz phase domain fluorometer at the Center for Fluorescence Spectroscopy, University of Maryland at Baltimore. An argon ion mode-locked laser (1 W at λ = 514 nm) was used as described in Methods. Na^+,K^+-ATPase (2 mg prot/ml) was labeled with ErITC (8 μM) in 50 mM Tris-HCl, 1 mM EGTA, pH 9.0 and lifetime measurement were made in 100 mM Tris-HCl, 2 mM EGTA, at pH 7.4 (1 mg/ml final concentration) under the same conditions. Symbols: τ_i values (1, 2, 3) are the calculated lifetime components, the α_i are the preexponential factors and f_i the fractional steady-state intensities, respectively. The average lifetime $\langle\tau\rangle$ was calculated as defined in the Methods section.

TABLE 4 **Determination of antiFITC antibody quenching of the fluorescence of enzyme bound and free FITC and ErITC**

	% Decrease in fluorescence intensity		
	Conformation of labeled Na^+,K^+ATPase		
Fluorescent probe	$Na^+ \cdot E_1$	$K^+ \cdot E_2$	Unbound probe in buffer
FITC	39 ± 5%	39 ± 3%	97 ± 2%
ErITC	1 ± 1%	1 ± 1%	0

The enzyme was labeled as described in Methods (FITC = 10 μM, ErITC = 8 μM) and the steady-state fluorescence intensities with λ_{ex} = 495 nm, λ_{em} = 520 nm for FITC, and λ_{ex} = 535 nm, λ_{em} = 558 nm for ErITC were measured in 10 mM Tris, 1 mM EGTA, 4 mM NaCl, pH 7.4, (final protein concentration 10 μg/ml). The $Na \cdot E_1 \langle\leftrightarrow\rangle K \cdot E_2$ conformational transition of the samples was evoked by the addition of 40 mM KCl (as the final concentration). The quenching of fluorescence intensity after addition of antiFITC antibody (5 μg/ml, final concentration) was recorded in percentage of quenching of the original intensity of the sample in E_1 conformation without antibody. The average values and standard deviations were calculated from four independent experiments.

intensity upon the $E_1 \rightarrow E_2$ transition very little if any change occurred for the ErITC-labeled enzyme. Also the ErITC-directed polyclonal antibodies that we raised did not quench the fluorescence of free ErITC, while FITC is efficiently quenched by anti-FITC antibodies. Furthermore, ErITC-Na^+,K^+-ATPase fluorescence was found to be poorly quenched by the iodide ion (K_q = 0.4 M^{-1} for ErITC-enzyme, versus K_q = 3.5 M^{-1} for FITC-enzyme). These results suggested that the quenching processes that occur as a result of the enzyme's conformational changes or upon antibody binding can strongly effect FITC, which has a fluorescence decay lifetime of ~3.5 ns but not ErITC, which has a lifetime of 0.35 ns.

Intra alpha distances: the determination of distances between the 5′-IAF/ErITC and AO/ErITC labeling, or binding sites on the alpha subunit. As shown in Fig. 2 the absorption spectrum of ErITC overlaps well with the emission spectrum of FITC. Because the fluorescein derivative 5′-IAF also has the same spectral properties as FITC, but it reacts with the enzyme's −SH rather than $-NH_2$ groups, we were able to measure the FET (or distance) between the 5′-IAF labeling site in the lamb enzyme at Cys-457 (Tyson et al., 1989), and at the ATP (and FITC) binding region labeled by ErITC. When we followed the iodoacetate pretreatment procedure of Kapakos and Steinberg (1986) to reduce nonspecific labeling we found a nearly stoichiometric incorporation of 5′-IAF (5.3 nmol/mg protein) into α. Next we found (Fig. 6 *a*) that the fluorescence intensity of the enzyme bound 5′-IAF was substantially reduced after the addition of ErITC. A 67 ± 3% decrease in the 5′-IAF emission and a new peak of sensitized ErITC emission at λ_{em} = 558 nm appeared. Due to the low quantum yield from ErITC, though, only the 5′-IAF donor fluorescence decrease was analyzed for the distance measurements. In addition, we were not able to simply use the observed efficiency of FET and the calculated R_0 (Forster radius) value to determine the apparent distance between the probes. This was because not all of the ErITC (or FITC) labeling occurs at the conformation sensitive, or putative ATP binding site (Abbott et al., 1991), and because we found that the 5′-IAF labeling procedure reduced total FITC or ErITC labeling. This problem was solved by taking advantage of the fact that anti-fluorescein antibodies almost completely quenched the fluorescence of both the enzyme bound 5′-IAF (Fig. 6 *a*, *inset*) and the nonspecifically bound FITC. We incubated both the 5′IAF-Na^+,K^+-ATPase and nonlabeled Na^+,K^+-ATPase with FITC and measured their fluorescence intensities before and after addition of antifluorescein antibody. The ratio of the remaining fluorescence in the doubly-labeled- to single-labeled proteins approximated the fraction of site-specific labeling present in the double (5′-IAF & FITC) labeled sample. This fraction was f = 0.70. Thus the 5′IAF labeling reduced the specific FITC labeling to

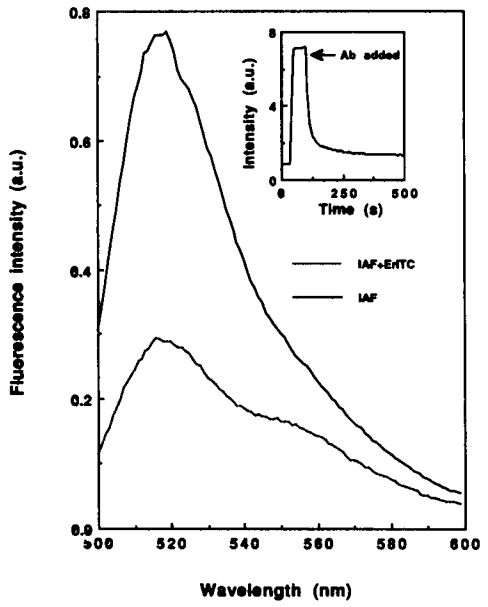

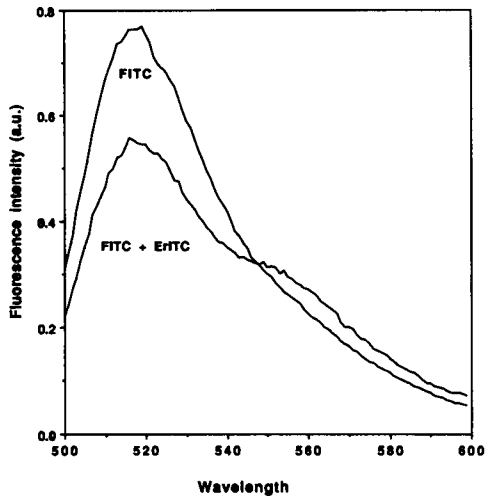

FIGURE 6 (*a*) (*Top*) The fluorescence emission spectra of enzyme bound 5′-IAF in the absence and presence of ErITC labeling. The upper (*solid line*) curve shows the emission spectra of Na^+,K^+-ATPase bound 5′-IAF and the lower curve (*dotted line*) the 5′-IAF spectra subsequent to the protein's labeling with ErITC (8 μM). The enzyme was labeled as described in Methods and corrected emission spectra were taken (λ_{ex} = 485 nm). The final protein concentration was 5 μg/ml. (*Inset*) Time course of 5′-IAF fluorescence quenching due to the addition of antibodies directed against fluorescein. The final concentration of the antibody was 10 μg/ml. (*b*) (*Bottom*) The steady-state fluorescence emission spectrum of FITC-labeled and FITC/ErITC doubly-labeled Na^+,K^+-ATPase. The upper curve shows the emission spectra of the FITC-labeled enzyme (50% inhibited with FITC, see Results) before, and the lower curve after labeling by ErITC (8 μM). The FITC- and FITC, ErITC-Na,K-ATPase (10 ug prot/ml) fluorescence emission spectra were taken at λ_{ex} = 490 nm.

70% of that of the single probe labeled enzyme. These results were then applied to the ErITC labeling work, and when the corrections were made (see Fortes and Aquilar, 1988) the calculated energy transfer efficiency increased from 67 to 97%. Next we found that in contrast to the high anisotropy values of ErITC and FITC, the r value for 5′-IAF ($r = 0.170 \pm 0.005$) was sufficiently low that we used the orientation factor $K^2 = 2/3$ (Haas et al., 1978) in making the distance calculations. Using the corrected energy transfer value of 97% and the calculated R_0 value (Table 5) we estimated the distance between the two sites as R_0 = 3.2 nm. This correlates rather well with the R_0 = 2.4 mm distance value calculated previously by Fortes and Aquilar (1988) between 5′-IAF and TNP-ATP on the α subunit of the dog kidney enzyme. Interestingly, we also found that the 5′-IAF labeled lamb kidney enzyme, unlike the dog but like the pig enzyme (Steinberg and Karlish, 1989), shows no fluorescence intensity responses to $E_1 \leftrightarrows E_2$ conformational transitions (data not shown).

AO and ErITC. ErITC was also a convenient probe to use for the determination of the distance between anthroylouabain (AO) and the ATP binding site because it has a significant spectral overlap with AO. In these determinations we made no stoichiometry corrections because AO only binds to active enzyme and we found that its anisotropy (r = 0.17) was low enough for us to use the standard orientation factor value of $K^2 = 2/3$. The AO donor fluorescence intensity decreased ~5% due to labeling with ErITC which generated a calculated R = 7.2 nm, a value which was similar to that observed previously with AO and FITC (Carilli et al., 1982; Abbott et al, 1991).

Alpha-Alpha interactions: characterization of the Forster energy transfer between ErITC- and FITC-labeled enzyme. In these experiments we labeled Na^+,K^+-ATPase with a

TABLE 5 The calculated values of Forster distance (R_0) and critical (R_c), and separation distances (R) between donor/acceptor pairs on the Na^+,K^+-ATPase

Donor/acceptor pair	R_0 (nm)	R_c (nm)	R
FITC/ErITC	6.2	6.2	5.6
FITC/TNP-ATP	3.2	3.6	5.5
AO/ErITC	4.4	4.7	7.2
5-IAF/ErITC	5.8	6.2	3.2

The Na,K-ATPase was labeled with individual donor or acceptor, respectively, as described in Methods. The absorption spectra, respective fluorescence quantum yields and emission spectra were taken and both the Forster R_0 and critical R_c distances were calculated as given in the Methods Section. The R_0 value for FITC/ErITC was calculated as described in the Results section with the orientation factor K^2 = 1.0, while all other R_0 values used $K^2 = ⅔$.

concentration of FITC (~4nmol/mg enzyme), which achieved ~50% inhibition and a 0.5 molar labeling ratio, and then labeled with 8 μM ErITC. After removal of unbound probe at each step we then measured the fluorescence decay lifetime of enzyme-linked FITC in the absence and presence of ErITC labeling. These measurements (made using an ISS modified SLM 4800 fluorometer) gave $\tau = 3.6 \pm 0.3$ ns and $\tau = 2.6 \pm 0.2$ ns values, respectively. Best fits to the data, as demonstrated by minimum values of the "goodness of fit" parameter ($\chi^2 = 4$ for FITC-NKA and $\chi^2 = 6$ for FITC, ErITC-NKA), was achieved with a two lifetime component fit. A short 10 ps, small fractional (20%) component, which was attributed to light scattering by the samples, and the larger value as given above attributed to FITC itself. The decreased lifetime for FITC on the double-labeled enzyme clearly indicated the presence of energy transfer with an efficiency of ~28%.

In addition to the lifetime measurements we also determined the energy transfer by measuring the altered steady-state fluorescence intensity. This method is quicker and uses considerably less enzyme. The exposure of the enzyme to intense light sources is also much shorter and causes less damage to the enzyme. Using this approach we found the FITC donor fluorescence ($\lambda_{max} = 520$ nm) to be reduced ~39% while a shoulder of sensitized ErITC emission at $\lambda = 558$ nm appeared (see Fig. 6 *b*).

It is important to note that neither the FITC/ErITC, nor the 5'-IAF/ErITC donor/acceptor pairs showed any change in the donor fluorescence quenching or energy transfer upon ligand-induced transition of the enzyme between the Na^+E_1 and K^+E_2 conformations.

Solubilization experiments. Solubilization of the enzyme by SDS provided additional evidence that intermolecular Forster energy transfer was occurring. In these experiments both FITC-labeled and FITC, ErITC doubly-labeled enzyme were titrated with increasing SDS concentrations and the steady-state fluorescence intensity of the probes was monitored along with their anisotropies. Fig. 7 shows that the doubly-labeled enzyme showed a much smaller decline in FITC fluorescence than did the FITC only preparation. The efficiency of FET decreased from ~40 to 10% upon enzyme solubilization, and this was accompanied by a substantial drop in FITC anisotropy. These changes in FITC properties were also directly correlated with the decrease in enzyme activity observed upon the addition of SDS to active, unlabeled enzyme. The fluorescence of ErITC also decreased slightly, while its anisotropy, because of its short lifetime, did not change (data not shown).

The specificity of energy transfer. After demonstrating that the two probes competed with each other's covalent

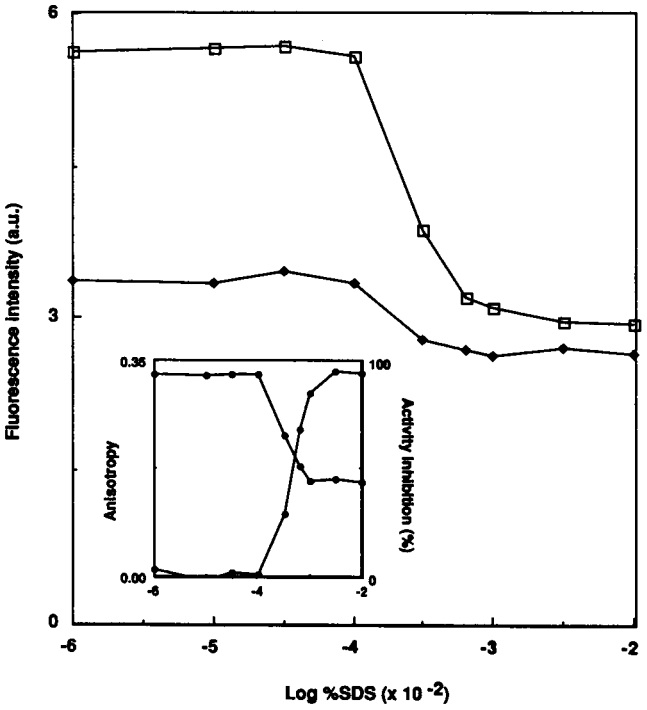

FIGURE 7 Determination of the effect of SDS solubilization upon Forster energy transfer from FITC to ErITC. The fluorescence intensity of FITC-Na^+,K^+-ATPase (□) and doubly labeled FITC/ErITC-Na^+,K^+-ATPase (◆) in 50 m*M* Tris-HCl, 1 mM EGTA, pH 7.4 upon addition of increasing concentrations of SDS. The protein concentration was 5 μg/ml, with the excitation wavelength ($\lambda_{ex} = 490$ nm, and emission wavelength, $\lambda = 535$ nm. Enzyme labeling, as in Fig. 6 *b*. (*Inset*) The decrease in steady-state anisotropy (r) of FITC-Na^+,K^+-ATPase (○) was measured under the same conditions as mentioned above while the activity of unlabeled enzyme (●) is shown as a function of increasing concentrations of SDS.

labeling at the ATP site, we also established that this same labeling competition was observed in the monitoring of FET. Fig. 8 shows the effect of varying the concentration of FITC used for the initial labeling while the subsequent labeling concentration of ErITC (8 μM) was held constant. This data shows that the extent of FET (as a percent of maximum quenching) is maximal at low FITC labeling concentrations and then decreases to a value that is ~20% of the maximum (39% FET) as the FITC concentration exceeds 10 μM. This is consistent with the two probes competing for the same high affinity site. In addition, maximal FET occurs in the region where the FITC labeling causes ~40% inhibition of enzyme activity. Maximal energy transfer occurs at low FITC concentrations because the probability of the ErITC acceptor occupying a neighboring ATP binding site is relatively high, while at high FITC concentrations few labeling sites remain. As with the solubilization ex-

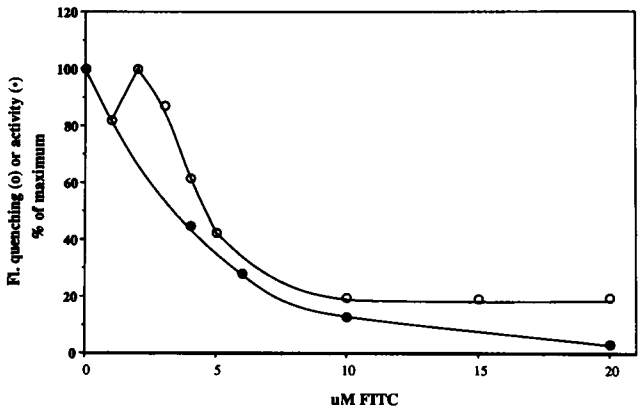

FIGURE 8 Effect of FITC labeling on fluorescence energy transfer. Na^+,K^+-ATPase was labeled initially with 0–20 μM FITC and subsequently with 8 μM ErITC. Energy transfer was measured as the ErITC induced quenching of FITC fluorescence. The data (○) are normalized relative to the maximum level of FET observed (39%). The concentration dependence of ATPase activity inhibition by FITC (from Table 1) is shown (●).

periments these data also indicate the presence of some nonspecific fluorescence energy transfer. Corrections for this transfer and the existence of unpaired donor and acceptors are dealt with in the following section.

Calculation of the energy transfer distance between FITC and ErITC. In order to make a reasonable estimation or calculation of the distance between the two probes we needed to either eliminate or identify and subtract out energy transfer that occurred due to probe not residing at the ATP site. We also needed to take into account the high degree of restriction in the rotational motions of both FITC and ErITC. We were able to eliminate nonspecific FITC labeling by adding the anti-FITC antibody. This antibody has been shown to quench the fluorescence of the population of enzyme-linked FITC that is not sensitive to conformational changes of the protein. Upon addition of antibody to the doubly-labeled preparation, the FITC fluorescence was decreased by 36% and the observed relative efficiency of FET increased from 40 to 63%. In order to be able to directly subtract the contribution of nonspecific ErITC labeling to the FET value, we derived the energy transfer rates taking into consideration both the labeling stoichiometry and proportions contributed by both the specific and nonspecific labeling populations. If we consider the case where FITC labels 0.5 mol % or less of the active enzyme, the rate of energy transfer from donor to acceptor, K_x, is given by:

$$K_x = p_n k_1 nF + k_2(nE - n_1 + nF), \quad (11)$$

where k_1 is the rate of energy transfer between the site specific labeling probes, while k_2 is the transfer between specifically bound FITC (the antibodies have quenched the nonspecific FITC population) and nonspecifically bound ErITC. The average molar ratio of bound FITC is given by nF, while nE is the molar ratio of specifically bound ErITC, n_1 is the number of ATP binding sites per Na^+,K^+-ATPase dimer (assuming an $\alpha_2\beta_2$ dimer with MW ≈ 270 kD), and p_n is the probability of Forster energy actually occurring. Assuming that FITC labels the enzyme population randomly, the maximum probability for transfer between FITC and ErITC was $p_n = 0.5$ when one-half of the enzyme molecules were labeled by FITC. This means that the observed energy transfer, occurring when ATPase activity is initially inhibited 50% by FITC, represents only one-half of the theoretical maximum. To calculate nF, we determined the concentration of protein bound FITC (cF) based upon its measured fluorescence relative to an FITC-Na^+,K^+-ATPase absorption standard. In the same samples we also determined the concentration of ouabain binding sites (cAO) by titrating the enzyme with AO and calculating:

$$nF = cF/cAO = 1.62, \quad (12)$$

assuming that specific FITC labeling occurs only on active enzyme. The concentration of ErITC was calculated relative to the total molar concentration of Na^+,K^+-ATPase (cT) because it appeared to label both native and inactive protein. In this case:

$$nE = cE/cT = 1.65, \quad (13)$$

where cE is a molar concentration of bound ErITC. When the enzyme was labeled by FITC and then by ErITC in the presence of ATP, we assumed that the observed energy transfer was occurring between FITC and nonspecific labeling ErITC. In this case the rate of energy transfer simplified to:

$$K_{nsp} = k_2 n'E = 0.28\ ns^{-1}, \quad (14)$$

where $n'E$ is the average number of unspecifically bound ErITC per dimer ($n'E = 2.5$). With the appropriate substitutions, the rate of energy transfer between the specific labeling fractions of the two probes is:

$$k_1 = K_x/(p_n nF) - K_{nsp}(nE - n_1 + nF)/(n'Ep_n nF), \quad (15)$$

and calculation of the results from three experiments gave us the average value for $k_1 = 0.51\ ns^{-1}$ and an efficiency of Forster energy transfer of $E = 0.65$. This value is only slightly larger than the value obtained after elimination of nonspecific FITC fluorescence ($E = 0.63$). This is probably because of off-setting effects with the

probability of energy transfer being inversely related to the energy transfer due to nonspecific labeling.

Calculation of orientation factor. In addition to the problem of identifying the extent to which nonspecific labeling contributed to the energy transfer, the other factor considered was the limitation placed on the energy transfer events as a result of the orientation of the donor and acceptor molecules. In theory, the uncertainty in their orientations can lead to fairly large errors in the calculated distance (Dale and Eisinger, 1976). In most cases though it is assumed that both donor and acceptor have substantial rotational freedom or they are able to depolarize during the lifetime of the donor's excited state. This is clearly not the case with FITC and ErITC. While we are not able to determine a true extent of ErITC immobilization because of its short fluorescence decay half-life, our determined anisotropy value for FITC on the enzyme is rather close to the maximum r_0 value determined for the probe in frozen solution (0.37 by Lakowicz et al., 1985). We therefore designed a simple model in order to determine the probable orientation factor K^2 values. We started with the basic Dale and Eisinger (1974) equation:

$$K^2 = [(\mathbf{a} \times \mathbf{b}) - 3(\mathbf{r} \times \mathbf{a})(\mathbf{r} \times \mathbf{b})]^2, \quad (16)$$

where **a** and **b** are unit vectors along the transition dipole directions of the donor and acceptor and **r** is the vector connecting vectors **a** and **b** (see Fig. 9). We then set specific constraints on the vectors. We have assumed that the orientation of both probes with respect to the α subunits is the same, and that the reorientation of each subunit is strictly by rotation around an axis perpendicular to the plane of the membrane into which each subunit is embedded. The orientations of both the donor and acceptor can then be described by α which is the angle between vectors **a** and **b** and their perpendicular projection onto the plane of the membrane (see Fig. 9). Angles β_1 and β_2 represent the angles of rotation of the perpendicular projections of vectors **a** and **b** in the plane of the membrane. After the appropriate operations the following equations can be used:

$$(\mathbf{a} \times \mathbf{b}) = 1 - \cos^2\alpha[1 - \cos(\beta_1 - \beta_2)] \quad (17)$$

$$(\mathbf{r} \times \mathbf{a}) = \cos\alpha \cos\beta_1 \quad (18)$$

$$(\mathbf{r} \times \mathbf{b}) = \cos\alpha \cos\beta_2. \quad (19)$$

Substitution of Eqs. 19–21 into Eq. 18 and application of standard trigonomic identities yields the dependence of the orientational factor upon the angles β_1, β_2, and α

$$K^2 = [1 - \cos^2\alpha[1 + \cos(\beta_1 + \beta_2) + \cos\beta_1 \cos\beta_2]]^2. \quad (20)$$

The value of the orientation factor was then calculated over all allowed angular combinations of the three angles at one degree increments and the frequency distribution of the possible K^2 values is shown in Fig. 10. Given the relatively similar orientations for both acceptor and donor molecules and their high degree of rotational restriction, we clearly cannot assume that $K^2 = 2/3$ but rather that K^2 can be any value from 0 to 4, with the most probable value found to be $K^2 = 1$.

After calculating the efficiency of energy transfer occurring between the specific labeling populations of FITC and ErITC as described and using $K^2 = 1$ to calculate R_0, the distance between ATP binding sites was calculated as $R = 5.6$ nm (Table 5). However, since the K^2 value is not actually known, we would calculate that it is 95% probable that the distance is shorter than 6.6 nm and 95% probable that the distance is greater than 3.3 nm.

Energy transfer between FITC and TNP-ATP.

As additional evidence to corroborate the conclusions of the FITC/ErITC experiments, we also measured the distance between the ATP binding sites by using FITC and TNP-ATP as a donor/acceptor pair. Again, approximately one-half of the ATP sites were labeled with FITC and then the fluorescence before and after addition of TNP-ATP was determined (in the presence of anti-FITC antibody). The observed efficiency of transfer was slightly less than 2%, but since we assume that FITC labeling is random and that only one-half of the molecules can contribute to energy transfer between FITC and TNP-ATP, an efficiency of Forster energy transfer value of 3% was derived. Using the short $R_0 = 3.3$ nm value characteristic of this pair of fluorophores and a $K^2 = \frac{2}{3}$ orientation factor (because TNP-ATP is not chemically linked to the enzyme), we calculated a distance of 5.5 nm between adjacent sites. This value is in good agreement with the value obtained using the FITC/ErITC pair. It is less accurate though because of the small extent of transfer observed, and the simplified calculation.

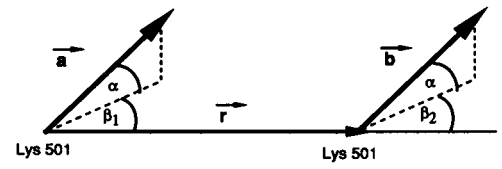

FIGURE 9 A model of the spacial orientation of the FITC emission dipole (unit vector $\hat{\mathbf{a}}$) relative to the ErITC absorption dipole (unit vector $\hat{\mathbf{b}}$) when separated by unit vector $\hat{\mathbf{r}}$ (Dale and Eisinger, 1974). In doubly labeled Na^+,K^+-ATPase heterodimer $(\alpha\beta)_2$ vectors **a** and **b** are assumed to form the same angle (α) relative to the plane of the membrane but have different rotational orientations (β_1 and β_2) relative to $\hat{\mathbf{r}}$.

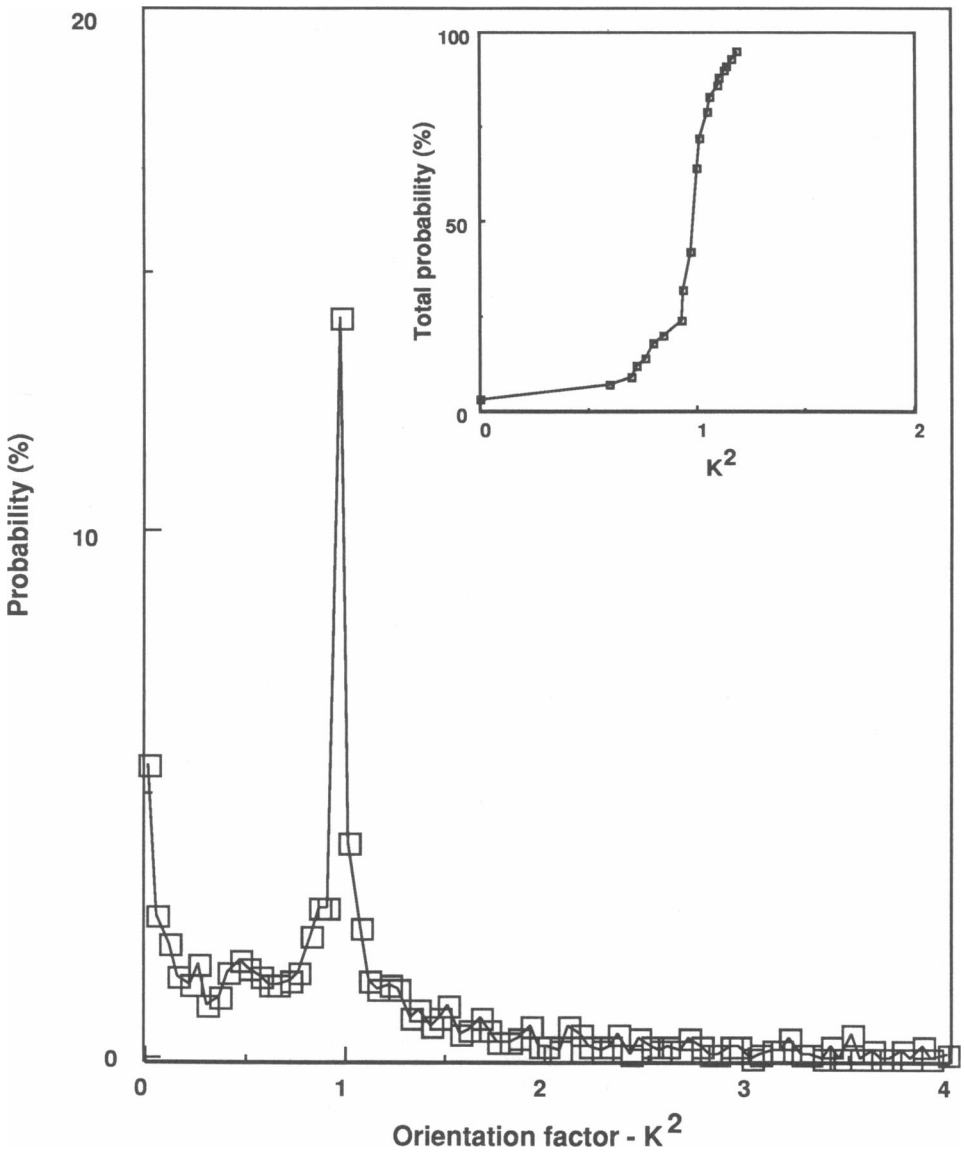

FIGURE 10 The calculated probability distribution of the orientation factor K^2 values. The probability was calculated according to Eq. 20 and was normalized to 1. (*Inset*) The probability function was integrated over the value range in order to depict the probability of the orientation factor being the value plotted on the ordinate.

DISCUSSION

The ligand-induced fluorescence intensity changes undergone by Na^+,K^+-ATPase-bound FITC are generally considered to reflect the conformational transitions undergone at the ATP binding region. In this work we took advantage of the fact that ErITC is a fluorescein derivative with the same isothiocyanate reactive group, therefore it could be expected to have similar properties. Indeed both compounds inactivated the enzyme at low concentrations and this inactivation was protected significantly by the presence of μmolar concentrations of ATP. This suggested that both probes occupy the high affinity adenine-binding pocket of the enzyme even though their sites of covalent labeling might not necessarily be identical because recent studies suggest that FITC may label other nearby Lys residues in addition to Lys-501 (Xu, 1989).

Our work further showed that both probes are capable of reducing each other's labeling by ~50% and that excess FITC abolished the ErITC labeling that serves as the FET acceptor. In addition, upon reaction with the enzyme, both probes show changes in their relative

quantum yields that suggest that a significant portion of their labeling is occurring at a nonpolar, hydrophobic site that is rather restricted in terms of its solvent access. Both probes also had additional, nonspecific labile sites of reaction that were not protectable by ATP. The major differences between the two probes are: (*a*) whereas enzyme linked-FITC undergoes significant fluorescent intensity changes upon ligand binding (up to 40% of the total fluorescence intensity), ErITC showed little or no change (less than 1%); (*b*) the fluorescence decay lifetime of FITC is not significantly altered by reaction with the enzyme while ErITC's is lengthened 3.8-fold; (*c*) ErITC has significantly lower Stern-Volmer quenching constants for fluorescence quenching by both KI and acrylamide; (*d*) the apparent anisotropy of ErITC was higher than that of FITC and no difference was found in the anisotropy values of the nonspecific and specific labeling fractions; and (*e*) SDS solubilization of the enzyme did not alter the anisotropy of ErITC. Most of these differences, however, may simply reflect the short lifetime for the decay of fluorescence of ErITC. Actually, taking the lifetime differences into account, the bimolecular quenching constants derived from the Stern-Volmer iodide quenching constants were similar for both FITC and ErITC. Similarly, little depolarization of ErITC could be expected to occur during its decay lifetime. Thus, while the large critical distance of the FITC/ErITC pair makes these two molecules extremely suitable for the investigation of energy transfer distances, the picosecond lifetime of ErITC fluorescence makes it unsuitable to study the Na^+,K^+-ATPase conformational changes or nanosecond motions. Its phosphorescence properties, though, have been investigated by Birmachu and Thomas (1989) as a means of analyzing protein motions and interactions of the sarcoplasmic reticulum Ca^{2+}-Mg^{2+}-ATPase enzyme that occur on the millisecond time scale.

An inconsistency in our results, though, is that because the ligand-induced intensity changes of FITC seem to result from static quenching events rather than lifetime-dependent effects we might still have expected ErITC to respond to ligand binding events that alter FITC fluorescence.

The large R_0 value for the FITC/ErITC pair has however proved to be useful for the FET distance measurements. The calculated average distance value of 56 Å places the ATP sites of neighboring alpha subunits in fairly close proximity when analyzed in terms of what we currently know about the three-dimensional organization of the enzyme. Depending upon the type of experimental technique used, the diameter of an αβ monomer appears to be ~40–70 and 80–110 Å for the length perpendicular to the plane of the membrane, with 50 and 100 Å being the most likely distances in these two dimensions (Jørgenson, 1982; Herbert et al., 1990). Furthermore, gel filtration and radiation inactivation studies suggest that the enzyme functions in a dimeric $(\alpha\beta)_2$ state (Hayashi et al., 1989; Cavieres, 1988; Brotherus et al., 1983). Also, computer enhanced electron micrograph images of the two-dimensionally crystalized enzyme have shown an $(\alpha\beta)_2$ dimer as the smallest assymetrical unit of the crystal (Mohraz et al., 1987). These dimers have been reported either as symmetrical (Mohraz et al., 1987) or asymmetrical heteromonomers orientated (Beall et al., 1989) about an axis perpendicular to the membrane plane. In either case, the distance of 56 Å between ATP binding sites, which was calculated from our FET measurements, can be accomplished within these dimers. If the dimers are symmetrical, then the location of the labeling sites is limited to opposite sides of a circle (diameter 56 Å) centered at the symmetry axis. In this model, the FITC/ErITC labeling site lies either in the interior of the protein mass or on the edge of a monomer near the monomer–monomer interface. We favor the interior location, however, because the FITC/ErITC labeling site has been shown to be in a rather inaccessible pocket (Abbott, et al. 1991). In addition, we have monitored the decays of anisotropy for both probes and we have found little detectable segmental motion for this region of the protein. Certainly the protrusions or "commas" farthest from the center of each α are too distant for the observed energy transfer (see Fig. 11 *a*). Interestingly, the comma contains the binding site of the monoclonal antibody M10-P5-C11, which inhibits the transfer of phosphate from ATP to Asp-369 of the lamb kidney enzyme (Ting-Beall et al., 1990; Ball, 1986). These data suggest that the comma region contains the site for phosphorylation while ErITC and FITC reside within the ATP binding site.

Putting the ATP site in the middle of the cytoplasmic mass of α is also consistent with our AO/ErITC distance measurement of 72 Å. Because the ouabain binding site is on the extracellular surface, and assuming the membrane to be 40 Å thick, the ATP binding site must be ~30 Å away from the cytoplasmic face of the membrane. This is only half of the (60 Å) distance from the membrane to the outermost edge of α as observed with the crystalized enzyme (Mohraz, et al., 1987). Inspection of the three-dimensional model of Na^+,K^+-ATPase constructed from electron micrographs shows the comma to also be ~30 Å from the intracellular membrane. These considerations suggest that the cross-sectional shape of the Na^+,K^+-ATPase dimer 30 Å from the membrane can be divided into an inner, ATP binding domain, and an outer, phosphorylation, domain as illustrated in Fig. 11 *B*.

We would then place the 5′-IAF site at an exposed, highly solvent accessible position on the intracellular

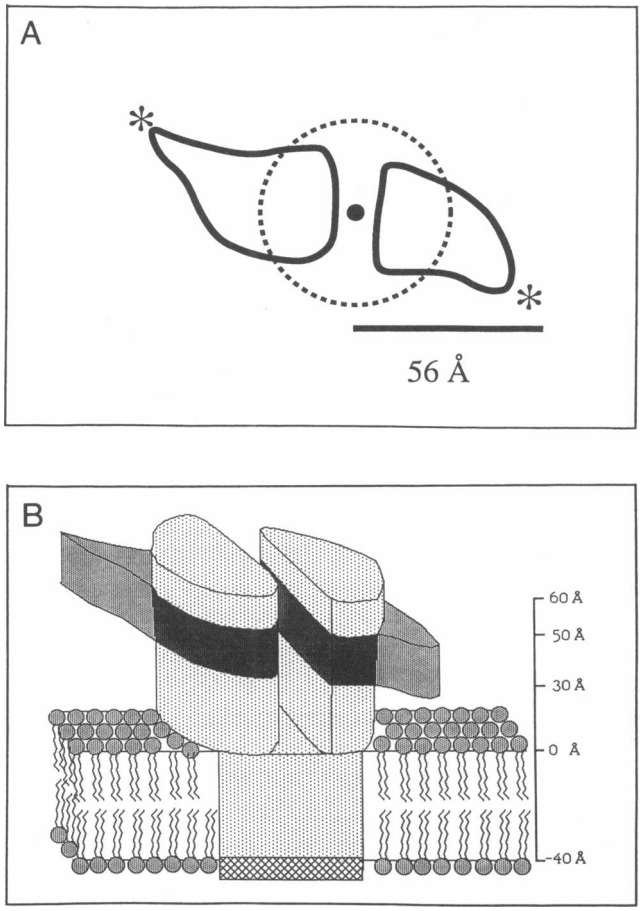

FIGURE 11 A model depicting the distances and locations of the ATP and antibody M10-P5-C11 binding regions on the alpha-subunit of Na^+,K^+-ATPase. *A* Shows an outline of the two-dimensional image of the cytoplasmic portion of the Na^+,K^+-ATPase dimer as obtained from electron micrographs of the negatively stained enzyme and the location (*) of the mAb M10-P5-C11 binding sites (Ting-Beall et al., 1990). The possible locations of the ATP binding sites in the symmetrical dimer and 56 Å apart lie on the overlayed dotted line. *B* Shows a model based upon a three-dimensional reconstruction by Mohraz (1987) and energy transfer measurements (herein; Carilli et al., 1982). Both mAb and ATP binding sites are 30 Å from the surface of the membrane. The darkest region is the nucleotide binding region, the grey "comma" domain is the antibody M10-P5-C11 epitope or phosphorylation site, and the cross-hatched region the cardiac glycoside binding domain.

side closer to the membrane and ~32 Å from ErITC. This should put it just about on the exposed surface of the protein with the cross-sectional diameter of α at this region being ~40–50 Å. Our results with the 5′-IAF/ErITC pair are in good agreement with the FET results obtained earlier by Fortes and Aquilar (1989), with 5′-IAF/FITC using the dog kidney enzyme. We were not, however, able to detect any conformation-dependent changes in 5′-IAF fluorescence intensity as reported by Kapakos and Steinberg (1986) for the dog enzyme. Therefore, we don't know whether the labeling on the lamb enzyme occurs at a site different from the dog enzyme or whether their respective labeling site environments are different but the relative distances from 5′-IAF to the FITC/ErITC labeling site seem similar.

Our results strongly suggest that an $(\alpha\beta)_2$ dimer is an organizational unit of Na^+,K^+-ATPase. Theoretically, there could still be alternative explanations: i.e., the observed energy transfer could occur between monomers mutually separated by only a thin layer of phospholipids. In our purified Na^+,K^+-ATPase preparation there is ~1.1 μmol phospholipid/mg protein (Lane et al., 1979), and this means that there are about four–five times more phospholipid present than the minimum number expected to comprise the annulus or motionally-restricted boundary population surrounding the protein (Essman, et al., 1985). It seems reasonable to assume that the lipids are randomly spread about the protein molecules and, thus, there would be a layer about five phospholipids deep about each αβ complex. Assuming ~5 Å as an appropriate diameter of one phospholipid molecule (Essman et al., 1985), this would mean that on the average ~50 Å (10 lipids) would separate each functional unit (provided that phospholipids were above the phase transition temperature). This would require the unlikely situation that the FITC/ErITC binding sites be on the outer surface of the alpha-subunit and rotationally oriented such that they are in the closest possible proximity. Thus, it seems reasonable to assume that $(\alpha\beta)_2$ dimers do exist as functional units within our membrane preparation.

In these studies we have dealt with two major difficulties that have not been considered in depth in previous energy transfer determination studies of the Na^+,K^+-ATPase. The first has to do with the high degree of rotational restriction of the fluorophores. The second has to do with the problems that arise when there is more than one labeling site on the enzyme for a fluorescent probe. A high degree of rotational restriction of the fluorophores makes it inappropriate to use an orientational factor of $K^2 = \frac{2}{3}$ in the calculation of distance between fluorophores from Forster energy transfer experiments (Dale and Eisinger, 1974). We find that the K^2 factor can range from between 0 to 4, for stationary donor/acceptor pairs of unknown mutual orientations. Thus, for any given experimental value of Forster energy transfer the actual distance between fluorophores could approach 0 or be more than six times longer than that calculated using the generally accepted value $K^2 = \frac{2}{3}$. For only partially restricted probes the $K^2 = \frac{2}{3}$ value is probably sufficiently accurate for energy transfer distance calculations (Haas et al., 1978). That

was, unfortunately, not our case since both FITC and ErITC were highly immobilized on the subnanosecond and nanosecond time scale. The differential tangent measured by frequency domain fluorometry was close to zero (data not shown; but not higher than 3 degrees) for both probes even when we measured rotational depolarization over a wide range of modulation frequencies (from 7 MHz up to 2 GHz for ErITC). We chose, therefore, a statistical approach to solve this problem. Our model should be generally applicable for the calculation of distances between immobilized donor and acceptor pairs that fulfill our following conditions: (*a*) the distance is calculated between two identical proteins (binding sites) embedded into the lipid bilayer; (*b*) both donor and acceptor have the same (or similar) orientation with respect to the protein. Clearly, the value $K^2 = 1$ is the most probable for this model. There is only a small probability that the calculated distance would be seriously underestimated. This results from the low probability of K^2 being greater than 1. A higher probability exists that R_0 could be shorter than our calculated value. The calculated probability that K^2 is near 0 is also relatively high, but this likelihood was experimentally diminished by the results obtained with the FITC/TNP-ATP donor/acceptor pair. Like FITC and ErITC, TNP-ATP is expected to bind at the ATP binding site. Although the rotational restrictions of TNP-ATP are unknown, it is highly probable that the emission dipoles of covalently bound ErITC and noncovalently bound TNP-ATP are not parallel. If the orientation factor for the FITC/ErITC pair was close to zero, the actual distance between them would be quite short. In that case, then, we should have also observed a high degree of Forster energy transfer with FITC/TNP-ATP. In fact the efficiency of Forster energy transfer for this pair was only ~3%, and this gave a calculated distance similar to that obtained using FITC/ErITC.

The second problem was the Forster energy transfer contribution of nonspecific labeling of the enzyme by both FITC and ErITC. The problem was resolved by combining two approaches. A polyclonal antibody population directed against FITC was used to quench the fluorescence of FITC that does not contribute to the conformational change-sensitive fluorescence signal. Because these antibodies do not cross-react with ErITC, we also raised antibodies to ErITC (coupled to KLH) only to find that the extremely short lifetime of this probe resulted in its not being amenable to antibody quenching. Therefore, we made use of the protective effect of ATP, and we measured the energy transfer occurring between FITC and ErITC when the second probe labeling was done in either the presence or absence of ATP. Thus, a corrected value for the energy transfer efficiency was obtained.

We thank Dr. Larry McLean (Marion Merrell-Dow, Cincinnati) for his help and use of the multi-frequency phase fluorometer (ISS1 SLM-4800), and Dr. Henryk Malak and Dr. Joseph Lakowicz (Center for fluorescence spectroscopy, University of Maryland School of Medicine, Baltimore) for their assistance with the experiments using the high frequency 10 GHz fluorometer system.

This work was supported by research grant HL-R01 32214 (to Dr. Ball) from the National Institutes of Health, and from the American Heart Association, an Ohio Affiliate Fellowship (to Dr. Abbott).

Received for publication and in final form 28 May 1991.

REFERENCES

Abbott, A., E. Amler, and W. J. Ball. 1991. Immunochemical and spectroscopic characterization of two fluorescein 5'-isothiocyanate labeling sites on Na^+,K^+-ATPase. *Biochemistry.* 30:1692–1701.

Ball, W. J. 1986. Uncoupling of ATP binding for Na^+,K^+-ATPase from its stimulation of ouabain binding: studies of the inhibition of Na,K-ATPase by monoclonal antibody. *Biochemistry.* 25:7155-7162.

Beall, H. C., D. F. Hastings, and H. P. Ting-Beall. 1989. Digital image analysis of two-dimensional Na,K-ATPase crystals: dissimilarily between pump units. *J. Microsc.* 154:71–82.

Birmachu, W., and D. D. Thomas. 1990. Rotational dynamics of the Ca-ATPase in sarcoplasmic reticulum studied by time-resolved phosphorescence anisotropy. *Biochemistry.* 29:3904–3914.

Brotherus, J. R., L. Jacobson, and P. L. Jorgensen. 1983. Soluble and enzymatically stable (Na^+,K^+)-ATPase from mammalian kidney consisting predominantly of promoter αβ-subunits. *Biochim. Biophys. Acta.* 731:290–303.

Carilli, C. T., R. A. Farley, D. M. Perlman, and L. C. Cantley. 1982. The active site structure of Na^+- and K^+-stimulated ATPase. *J. Biol. Chem.* 257:5601–5606.

Cavieres, J. D. 1988. Association of biochemical functions with specific subunit arrangements in purified Na,K-ATPase. *In* The Na^+,K^+-Pump. J. C. Skou, J. G. Norby, A. B. Maunsbach, and M. Esmann, editors. Part A. Alan R. Liss, New York. 175–180.

Dale, R. E., and J. Eisinger. 1974. Intramolecular distances determined by energy transfer dependence on orientational freedom of donor and acceptor. *Biopolymers.* 13:1573–1605.

Dale, R. E., and J. Eisinger. 1976. Intra molecular energy transfer and molecular conformation. *Proc. Natl. Acad. Sci. USA.* 73:271–273.

Esmann, M., A. Watts, and D. Marsh. 1985. Spin-label studies of lipid-protein interactions in Na^+,K^+-ATPase membranes from rectal glands of squalus acanthias. *Biochemistry.* 24:1386–93.

Farley, R. A., C. M. Tran, C. T. Carilli, D. Hawke, and J. E. Shively. 1984. The amino acid sequence of a fluorescein-labeled peptide from the active site of (Na^+,K^+)-ATPase. *J. Biol. Chem.* 259:9532–9535.

Forster, T. H. 1951. Fluorescenz Organischer Verbidungen. Vandehoeck & Ruprecht, Gottingen, Germany. p. 67.

Fortes, P. A. G. 1986. A fluorometric method for the determination of functional (Na^+,K^+)-ATPase and cardiac glycoside receptors. *Anal. Biochem.* 158:454–462.

Fortes, P. A. G., and R. Aquilar. 1988. Distances between 5'-iodoacetamidofluorescein and the ATP and ouabain sites of (Na^+,K^+)-ATPase determined by fluorescence energy transfer. *In* The Na^+, K^+-Pump. J. C. Skou, J. G. Nørby, A. B. Maunsbach, and M. Esmann, editors. Part A. 197–204.

Friedman, M. L., and W. J. Ball, 1989. Determination of monoclonal antibody-induced alterations in Na^+/K^+-ATPase conformations using fluorescein-labeled enzyme. *Biochim. Biophys. Acta.* 995:42–53.

Gingold, M. P., J. L. Rigaud, and P. Champeil. 1981. Fluorescence energy transfer between ATPase monomers in sarcoplasmic reticulum reconstituted vesicles. *Biochimie.* 63:923–925.

Haas, E., E. Katchalski-Katzir, and I. Z. Steinberg. 1978. Effect of the orientation of donor and acceptor on the probability of energy transfer involving electronic transitions of mixed polarization. *Biochemistry.* 17:5061–5070.

Hayashi, Y., K. Mimura, H. Matsui, and T. Takagi. 1989. Minimum enzyme unit for Na^+,K^+-ATPase is the αβ-promoter. *Biochim. Biophys. Acta.* 983:217–229.

Herbert, H., E. Skriver, U. Kaveus, and A. B. Maunsbach. 1990. Coexistence of different forms of Na^+,K^+-ATPase in two-dimensional membrane crystals. *FEBS Lett.* 268:83–87.

Jensen, J., and J. G. Nørby. 1989. Thallium binding to native and radiation-inactivated Na^+,K^+-ATPase. *Biochim. Biophys. Acta.* 985: 248–254.

Jesaitis, A. J., and P. A. G. Fortes. 1980. Fluorescence studies of the sodium and potassium transport adenosine triphosphatase labeled with fluorescein mercuric acetate and anthroylouabain. *J. Biol. Chem.* 255:459–467.

Jørgensen, P. L. 1982. Mechanism of the Na^+,K^+ pump: protein structure and conformations of the pure (Na^+ + K^+)-ATPase. *Biochim. Biophys. Acta.* 694:27–68.

Jørgensen, P. L., and J. P. Andersen. 1988. Structural basis for E_1-E_2 conformational transitions in Na^+,K^+-Pump and Ca^{2+}-pump proteins. *J. Membr. Biol.* 103:95–120.

Kapakos, J. G., and M. Steinberg. 1986. 5′-Iodoacetamido fluorescein-labeled (Na^+,K^+)-ATPase. *J. Biol. Chem.* 261:2090-2095.

Karlish, S. J. D. 1980. Characterization of conformational changes in (Na^+,K^+)ATPase labeled with fluorescein as the active site. *J. Bioenerg. Biomembr.* 12:111–136.

Laczko, G., I. Gryczynski, Z. Gryczynski, W. Wiczk, H. Malak and J. R. Lakowicz. 1990. A 10-GHz frequency-domain fluorometer. *Rev. Sci. Instrum.* 61:2331–2337.

Laemli, U. K. 1970. Cleavage of structural proteins during the assembly of the head of bacterialphage T4. *Nature (Lond.).* 227:680–685.

Lakowicz, J. R. 1983. Principles of fluorescence spectroscopy. Plenum Press, New York. pp. 305–337.

Lakowicz, J. R., M. Cherek, B. P. Maliwal, and E. Gratton. 1985. Time-resolved fluorescence anisotropies of diphenylhexahiene and perylene in solvents and lipid bilayers obtained from multifrequency phase-modulation fluorometry. *Biochemistry.* 24:376–383.

Lakowicz, J. R., G. Laczko, H. Cherek, E. Gratton, and M. Limkeman. 1984. Analysis of frequency decay kinetics from variable-frequency phase shift and modulation data. *Biophys. J.* 46:463–477.

Lane, L. K., J. D. Potter, and J. H. Collins. 1979. Large-scale purification of Na,K-ATPase and its protein subunits from lamb-kidney medulla. *Prep. Biochem.* 9:157–170.

Lee, J. A., and P. A. G. Fortes. 1986. Spatial relationship and conformational changes between the cardiac glycoside site and β-subunit oligosacharides in sodium plus potassium activated adenosinetriphosphate. *Biochemistry.* 25:8133–8141.

Lowry, O. H., N. J. Rosebrough, A. L. Farr, and R. J. Randall. 1951. Protein measurement with the Folin phenol reagent. *J. Biol. Chem.* 193:265–275.

McDonough, A. A., K. Geering, and R.A. Farley. 1990. The sodium pump needs its β subunit. *FASEB J.* 4:1598–1605.

McLean, L. R., J. L. Krstenansky, T. J. Owen, M. R. Eftink, and K. A. Hagaman. 1989. Effect of micelle diameter on tryptophan dynamics in an amphipathic helical peptide in phosphatidylcholine. *Biochemistry.* 28:8403–8410.

Moczydlowski, E. G., and P. A. G. Fortes. 1981. Characterization of 2′,3′-0-(2,4,6-trinitrocyclohexadienylidine) adenosine 5′-triphosphate as a fluorescent probe of the ATP site of sodium and potassium transport adenosine triphosphate. *J. Biol. Chem.* 256:2346–2356.

Mohraz, M., V. Simpson, and P. R. Smith. 1987. The three dimensional structure of the Na,K-ATPase from electron microscopy. *J. Cell. Biol.* 105:1–8.

Nørby, J. G., and J. Jensen. 1989. A model for the stepwise radiation inactivation of the α_2 dimer of Na,K-ATPase. *J. Biol. Chem.* 264:19548–19558.

Ottolenghi, P., and J. C. Ellory. 1983. Radiation inactivation of (Na^+,K^+)-ATPase, an enzyme showing multiple radiation-sensitive domains. *J. Biol. Chem.* 258:14895–14907.

Pachence, J. M., I. S. Edelman, and B. P. Schoenborn. 1987. Low-angle neutron scattering analysis of Na,K-ATPase in detergent solution. *J. Biol. Chem.* 262:702–709.

Papp, S., S. Pikula, and A. Martonosi. 1987. Fluorescence energy transfer as an indicator of Ca^{2+}-ATPase interactions in sarcoplasmic reticulum. *Biophys. J.* 51:205–220.

Pedemonte, C. H., and J. H. Kaplan. 1990. Chemical modification as an approach to elucidation of sodium pump structure function relations. *Am J. Physiol.* 258 (Cell Physiol. 27): C1–C23.

Schwartz, A., J. C. Allen, and S. Harigaya. 1969. Possible involvement of cardiac Na^+,K^+-adenosine biophosphatase in the mechanism of action of cardiac glycosides. *J. Pharmacol. Exp. Ther.* 168:31–41.

Skriver, E., A. B. Maunsbach, and P. L. Jorgensen. 1981. Formation of two-dimensional crystals in pure membrane-bound Na^+,K^+-ATPase. *FEBS Lett.* 131:219–222.

Spencer, R. D., and G. Weber. 1969. Measurements of subnanosecond fluorescence lifetimes with a cross-correlation phase fluorometer. *Ann. NY Acad. Sci.* 158:361–376.

Steinberg, M., and S. J. D. Karlish. 1989. Studies on conformational changes in Na^+,K^+-ATPase labeled with 5-iodoacetamidofluorescein. *J. Biol. Chem.* 264:2726–2739.

Taniguchi, K., K. Tosa, K. Suzuki, and Y. Kamo. 1988. Microenvironment of two different extrinsic fluorescence probes in Na^+,K^+-ATPase changes out of phase during sequential appearance of reaction intermediates. *J. Biol. Chem.* 263:12943–12947.

Ting-Beall, H. P., H. C. Beall, D. F. Hastings, M. L. Friedman, and W. J. Ball. 1990. Identification of monoclonal antibody binding domains of Na^+,K^+-ATPase by immunoelectron microscopy. *FEBS Lett.* 265:121–125.

Tyson, P. A., M. Steinberg, E. T. Wallick, and T. L. Kirley. 1989. Identification of the 5′-iodoacetamidofluorescein reporter site on the Na^+,K^+-ATPase. *J. Biol. Chem.* 264:7216.

Watanabe, T., and G. Inesi. 1982. Structural effects of substrate utilization on the adenosinetriphosphatase chains of sarcoplasmic reticulum. *Biochemistry.* 21:3254–3259.

Zampighi, G., J. Kyte, and W. Freytag. 1984. Structural organization of (Na^+,K^+)-ATPase in purified membranes. *J. Cell Biol.* 98:1851–1864.

Xu, K.-Y. 1989. Any of several lysines can react with 5′isothiocyanate fluorescein to inactivate sodium and potassium ion activated Adenosine triphosphatase. *Biochemistry.* 28:5764–5772.